

# The Use of Magnetic Dilution To Elucidate the Slow Magnetic Relaxation Effects of a Dy<sub>2</sub> Single-Molecule Magnet

Fatemah Habib,<sup>†</sup> Po-Heng Lin,<sup>†</sup> Jérôme Long,<sup>†</sup> Ilia Korobkov,<sup>†</sup> Wolfgang Wernsdorfer,<sup>‡</sup> and Muralee Murugesu<sup>\*,†,§</sup>

<sup>†</sup>Department of Chemistry, University of Ottawa, 10 Marie Curie, Ottawa, Ontario, Canada K1N 6N5

<sup>‡</sup>Institut Néel, CNRS & Université J. Fourier, BP 166, 25 Avenue des Martyrs, 38042 Grenoble, France

<sup>§</sup>Centre for Catalysis Research and Innovation, 30 Marie Curie, Ottawa, Ontario, Canada K1N 6N5

**S** Supporting Information

**ABSTRACT:** The magnetic dilution method was employed in order to elucidate the origin of the slow relaxation of the magnetization in a Dy<sub>2</sub> single-molecule magnet (SMM). The doping effect was studied using SQUID and micro-SQUID measurements on a Dy<sub>2</sub> SMM diluted in a diamagnetic Y<sub>2</sub> matrix. The quantum tunneling of the magnetization that can occur was suppressed by applying optimum dc fields. The dominant single-ion relaxation was found to be entangled with the neighboring Dy<sup>III</sup> ion relaxation within the molecule, greatly influencing the quantum tunneling of the magnetization in this complex.

The observation of slow relaxation of the magnetization in the molecular complex Mn<sub>12</sub>Ac led to the discovery of single-molecule magnets (SMMs) in the mid 1990s.<sup>1</sup> Since then, a variety of SMMs have been synthesized as molecular counterparts to magnetic nanoparticles.<sup>2</sup> Indeed, SMMs are molecules that function as single-domain nanoscale magnetic particles by exhibiting magnetization-versus-field hysteresis whose coercivity below the blocking temperature increases with increasing sweep rate and decreasing temperature.<sup>1</sup> This behavior results from the combination of a large ground spin state (*S*) with a large uniaxial (Ising-like) magnetoanisotropy (*D*) and leads to a significant energy barrier to magnetization reversal (*U*). However, in practice, quantum tunneling of the magnetization (QTM) through the barrier via higher-lying *M<sub>S</sub>* levels of the spin manifold results in an effective barrier *U<sub>eff</sub>* < *U*, which is apparent by the observation of steplike features in the hysteresis loops.<sup>1</sup> Such a magnetization relaxation mechanism is well-understood for transition-metal SMMs but is hard to elucidate for polynuclear lanthanide systems. This is mainly due to a combination of several factors, such as the large magnetic anisotropy found in lanthanide ions, high tunneling rates, and the weak magnetic interactions between 4f ions.<sup>2c,3</sup> Therefore, understanding the origin of the relaxation modes observed in polynuclear 4f SMMs remains an exciting challenge.

Precisely modulating the concentration of dilution/doping is a useful method for controlling the electronic and magnetic properties of a material.<sup>4</sup> In molecular systems, only a handful of complexes for which the effect of doping on the magnetic properties was investigated have been reported.<sup>4d–g</sup> To our knowledge, elucidation of the slow relaxation of the magnetization

in doped polynuclear lanthanide complexes has not been explored. We believe that the strategy of doping a diamagnetic system with a paramagnetic ion can shed some light on the complex relaxation processes inherent in 4f SMMs. Moreover, by variation of the concentration of the dopant ion, effects such as QTM can be accurately modulated. With this in mind, we isolated a phenoxo-bridged centrosymmetric Dy<sub>2</sub> SMM that exhibits slow relaxation of the magnetization below 25 K.<sup>5</sup> Our aim was to use the dilution method to elucidate whether such behavior originates from relaxation of a single ion or a magnetically coupled system. Herein we report the first relaxation studies using SQUID and micro-SQUID measurements on a Dy<sub>2</sub> SMM diluted in a diamagnetic Y<sub>2</sub> matrix. The doping effect clearly indicated that the observed relaxation predominantly arises from the single-ion relaxation mode, which is affected by the weak intramolecular exchange-biased coupling between the Dy<sup>III</sup> ions.

Single crystals of diluted complexes were prepared by reacting *N,N*-3-bis(3-methoxysalicylidene)diethylenetriamine (H<sub>2</sub>valdien) (1 equiv) and Y(NO<sub>3</sub>)<sub>3</sub>·6H<sub>2</sub>O/Dy(NO<sub>3</sub>)<sub>3</sub>·6H<sub>2</sub>O in 95:5, 90:10, and 50:50 percentage ratios (0.125 mmol) in 9 mL of 2:1 MeOH/*N,N*-dimethylformamide followed by the addition of triethylamine (2 equiv). Single-crystal X-ray structures of pure isostructural Y<sub>2</sub> and Dy<sub>2</sub> complexes were obtained (Figure 1), however because of the similar ionic radii of Dy<sup>III</sup> and Y<sup>III</sup> ions, it was not possible to distinguish the metal ions in the crystal structures of the diluted samples. Packing arrangements for the Y<sup>III</sup> analogue are given in Figures S1–S3 in the Supporting Information; the intramolecular Y<sup>III</sup>···Y<sup>III</sup> distance and the intermolecular distance between closest Y<sup>III</sup> ions were found to be 3.76 and 10.56 Å, respectively. In order to establish the exact amount of Dy<sup>III</sup> dilution that had taken place in the Y<sup>III</sup><sub>2</sub> samples, we performed inductively coupled plasma (ICP) measurements, which allow trace concentrations of an element in a sample to be determined precisely. The obtained results of 5.31, 10.24, and 50.56% dysprosium dilution were in good agreement with the values of 5, 10, and 50% employed during the synthesis. The probabilities of observing different dinuclear species at different Dy<sup>III</sup> dilution percentages are given in Table 1.

In order to probe the slow relaxation of the magnetization and the quantum tunneling effects occurring in lanthanide SMMs,

**Received:** March 6, 2011

**Published:** May 12, 2011

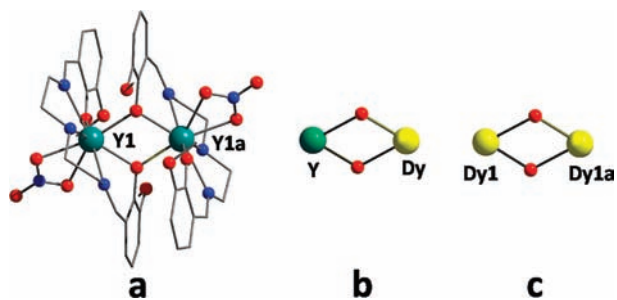


**Figure 1.** (a) Molecular structure of the centrosymmetric complex  $[Y_2(\text{valdien})_2(\text{NO}_3)_2]$  (1). (b) Core unit of the diluted YDy complex. (c) Core unit of the  $\text{Dy}_2$  complex. Symmetry-equivalent positions are denoted by an "a" in the label. Color code: yellow, Dy; green, Y; red, O; blue, N.

**Table 1. Calculated Probabilities of Observing Various Dinuclear Species at Particular  $\text{Dy}^{\text{III}}$  Dilution Percentages**

species	5% dilution	10% dilution	50% dilution
$Y_2$	0.9025	0.81	0.25
YDy	0.0950	0.18	0.50
$\text{Dy}_2$	0.0025	0.01	0.25

alternating current (ac) magnetic measurements were performed on crushed polycrystalline samples in the SQUID magnetometer, whereas the dc transverse field method using a micro-SQUID<sup>6</sup> was used for single crystals. The temperature dependence of the ac susceptibility in the 20–1.8 K range was measured for all of the diluted samples at various dc fields and frequencies (Figure 2 and Figures S4–S6). Initial measurements on diluted and nondiluted  $\text{Dy}_2$  samples under zero applied dc field exhibited a clear frequency-dependent signal below 20 K, indicating SMM behavior. A peak maximum was observed at  $\sim 10$  K for all samples, but below 6 K the tail of a frequency-dependent peak signal was observed for diluted samples (Figure 2, left). Such a tail of a peak is indicative of QTM through the spin-reversal barrier via degenerate  $\pm M_S$  energy levels.<sup>3b,4g,6</sup> Lanthanide ions are known to exhibit significant QTM, but in the case of  $\text{Dy}^{\text{III}}$  ions ( $^6\text{H}_{15/2}$ ,  $S = 5/2$ ,  $L = 5$ ,  $g = 4/3$ ), the QTM is reduced as a result of a spin-parity effect. The latter effect predicts that the QTM should be suppressed at zero field when the total spin of the magnetic system is a half-integer but allowed in integer-spin systems. However, QTM can be induced experimentally even in half-integer spin systems through effects such as environmental degrees of freedom as well as hyperfine and dipolar coupling via transverse field components.<sup>8</sup> The intensity of the tail increased with increasing percentage of Dy dilution, consistent with an increase in the major species YDy. This clearly demonstrates that the QTM seen in our system is consistent with mononuclear lanthanide SMMs exhibiting single-ion relaxation behavior.<sup>4g</sup>

In order to shortcut the QTM, it is possible to apply a static dc field while measuring the frequency-dependent signal. Indeed, in such measurements the degeneracy of the  $\pm M_S$  energy levels can be removed, consequently preventing the tunneling of electrons from the  $+M_S$  state through the spin-reversal barrier to the  $-M_S$  state. The thermal dependence of  $\chi''$  below 20 K at an applied dc field of 200 Oe (Figure 2, middle) exhibited a slight decrease in the tail observed below 6 K, confirming the latter assumption. It

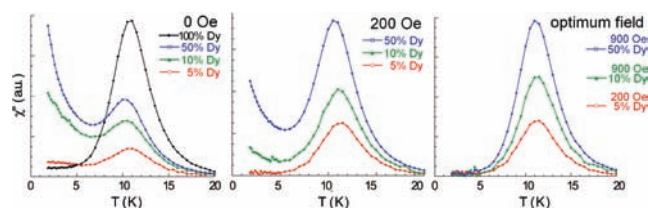


**Figure 2.** Temperature dependence of the out-of-phase susceptibility ( $\chi''$ ) at 250 Hz and applied fields of (left) 0, (middle) 200 Oe, and (right) the optimum field for the diluted samples.

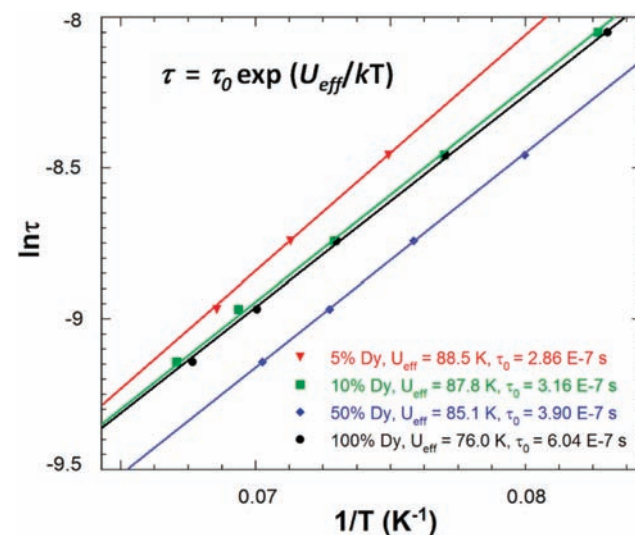


**Figure 3.** Plot of  $\ln(\tau)$ , where  $\tau$  is the relaxation time of the magnetization, vs  $1/T$  for all four samples. The effective energy barriers ( $U_{\text{eff}}$ ) obtained from the fits are indicated.

is noteworthy that there was only a slight shift of the peak maxima for all of the diluted samples. To fully suppress the tunneling effects, optimum dc field measurements were carried out at 10 K and optimum fields of 200, 900, and 900 Oe were found for 5, 10, and 50%  $\text{Dy}^{\text{III}}$  dilution, respectively. Subsequent ac measurements were carried out at these optimum fields (Figure 2, right), and a clear single-relaxation peak without the presence of a tail was observed in the out-of-phase plots, confirming the suppression of the QTM. The intensities of the peaks gave an indication that the major species present in the diluted samples was the YDy complex, consistent with the ICP data. The optimum-field data were used to derive Arrhenius plots (Figure 3), from which energy barriers ( $U_{\text{eff}}$ ) were extracted. The  $U_{\text{eff}}$  values of 88.5, 87.8, and 85.1 K obtained at 5, 10, and 50% dilution, respectively, are much larger than that of the parent 100%  $\text{Dy}_2$  complex (76.0 K). This trend demonstrates that the YDy species rather than the  $\text{Dy}_2$  species is the primary contributor to the relaxation barrier. Additionally, these results are consistent with those for previously reported dysprosium SMMs, in which the large relaxation barriers arise primarily from single-ion anisotropy.<sup>3c</sup> The obtained barriers are comparable to some of the largest barriers seen for transition-metal SMMs<sup>1b,2d</sup> but smaller than those for previously reported pure  $\text{Ln}^{\text{III}}$  SMMs.<sup>2c,3c</sup> The observed increase in the relaxation barrier with increasing magnetic dilution from 76.0 K for 100% Dy to 88.5 K for 5% Dy follows a similar trend reported previously by Jiang et al.<sup>4g</sup>

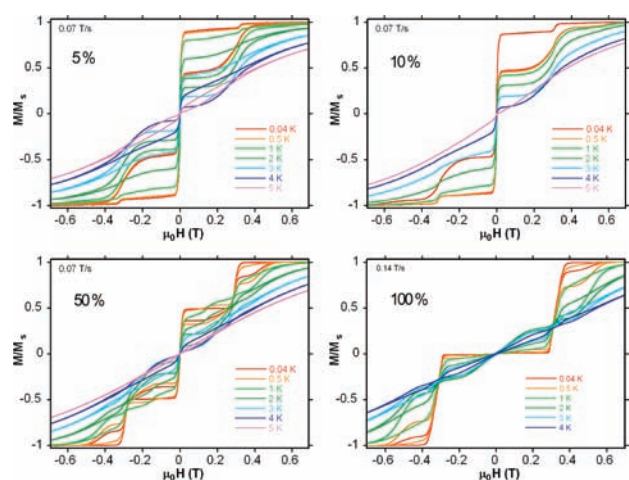


**Figure 4.** Field dependence of the normalized magnetization of samples containing (top left) 5, (top right) 10, (bottom left) 50, and (bottom right) 100% Dy between 0.04 and 5 K at the indicated sweep rates.

To further probe this dynamic behavior, single-crystal hysteresis loop measurements were carried out over the 0.04–5 K temperature range using a micro-SQUID. Hysteresis loops were measured on easy-axis-oriented single crystals of samples with 5, 10, and 50% dilution and compared to the data for the 100% Dy<sub>2</sub> complex (Figure 4). In the case of the 5%-doped sample (Figure 4, top left), a large step at zero field was observed. This is consistent with the QTM often observed for lanthanide systems.<sup>3</sup> Moreover, the latter behavior also confirmed the observed tail in the out-of-phase plot. As the field was increased, opening of the loop was observed, with the maximum opening occurring below 500 Oe, in agreement with the ac optimum field of 200 Oe. The latter observation clearly confirmed the suppression of QTM under an applied field. The small tunnel resonance step at ~0.3 T is due to the minor Dy<sub>2</sub> complex (Figure 1c), in which each Dy<sup>III</sup> ion acts as exchange-biased on its neighboring metal center within the molecule. This can be correlated to the step at 0.3 T for the 100% Dy sample, confirming its identity as the Dy<sub>2</sub> species. The magnitude of the small step due to Dy<sub>2</sub> can be compared with the large step due to YDy. The observed magnetization ratio of 1:19 is consistent with the presence of Dy<sub>2</sub>:YDy = 1:38, consistent with a dilution of 5%. Similar behavior was seen for the 10%-diluted sample, for which the observed magnetization ratio was 1:9, indicating a Dy<sub>2</sub>:YDy ratio of 1:18. At 50% dilution, the tunneling at zero field decreased, and the increased step at ~0.3 T (1:1 magnetization ratio) is indicative of the presence of 25% Dy<sub>2</sub> and 50% YDy (Figure 1b) species. In the 100% Dy<sub>2</sub> sample, the absence of the step at zero field indicates the absence of YDy species, which was responsible for the zero-field tunneling. The tunnel resonance step around ±0.3 T can be directly associated with the large spin flip of the antiferromagnetically coupled Dy<sup>III</sup> ions. The latter weak coupling (0.32 T) is comparable to that in the exchange-bias-coupled {Mn<sub>4</sub>}<sub>2</sub> system.<sup>9</sup> In previously reported transition-metal systems, the exchange-biased interactions originate mainly from weak intermolecular interactions via hydrogen bonds or dipolar interactions.<sup>9,10</sup> These interactions are sufficient in strength to perturb the QTM that occurs. In our system, the exchange-biased interaction is intramolecular in nature because of the weak coupling between the Dy<sup>III</sup> ions. In fact, 4f magnetic orbitals of lanthanide ions interact poorly with the bridging ligand orbitals

as a result of their core-orbital nature. Thus, the magnetic superexchange pathway via the ligand orbitals is less efficient.

In conclusion, the in-depth study of this diluted system clearly demonstrates that the slow relaxation of the magnetization originates from the single-ion relaxation of Dy<sup>III</sup> ions. However, this single-ion relaxation is entangled with the neighboring Dy<sup>III</sup> ion relaxation within the molecule via weak intramolecular exchange-biased interactions. This in turn suppresses the QTM at zero field that is generally observed for lanthanide systems. These results demonstrate the decisive role of the exchange interaction in such systems despite its small magnitude (typically less than 1 cm<sup>-1</sup>). This study further demonstrates that weak intramolecular exchange-biased interactions provide a novel approach for fine-tuning the QTM and understanding the nature of slow relaxation of the magnetization in SMMs. Finally, understanding the slow relaxation mechanism in 4f SMMs may pave the way forward toward the isolation of SMMs that can potentially be applied in the field of molecular electronics.

## ■ ASSOCIATED CONTENT

**S Supporting Information.** Complete experimental details and crystallographic data (CIF). This material is available free of charge via the Internet at <http://pubs.acs.org>.

## ■ AUTHOR INFORMATION

**Corresponding Author**  
m.murugesu@uottawa.ca

## ■ ACKNOWLEDGMENT

We thank the University of Ottawa, NSERC (Discovery and RTI Grants), CFI, and FFCR for financial support.

## ■ REFERENCES

- (1) (a) Sessoli, R.; Gatteschi, D.; Caneschi, A.; Novak, A. *Nature* **1993**, *45*, 141. (b) Sessoli, R.; Tsai, H.-L.; Schake, A. R.; Wang, S.; Vincent, J. B.; Folting, K.; Gatteschi, D.; Christou, G.; Hendrickson, D. N. *J. Am. Chem. Soc.* **1993**, *115*, 1804.
- (2) (a) Tasiopoulos, A. J.; Vinslava, A.; Wernsdorfer, W.; Abboud, K. A.; Christou, G. *Angew. Chem., Int. Ed.* **2004**, *43*, 2117. (b) Murugesu, M.; Habrych, M.; Wernsdorfer, W.; Abboud, K. A.; Christou, G. *J. Am. Chem. Soc.* **2004**, *126*, 4766. (c) Ishikawa, N.; Sugita, M.; Ishikawa, T.; Koshihara, S.; Kaizu, Y. *J. Am. Chem. Soc.* **2003**, *125*, 8694. (d) Milios, C. J.; Vinslava, A.; Wernsdorfer, W.; Moggach, S.; Parsons, S.; Perlepes, S. P.; Christou, G.; Brechin, E. K. *J. Am. Chem. Soc.* **2007**, *129*, 2754.
- (3) (a) Luzon, J.; Bernot, K.; Hewitt, I. J.; Anson, C. E.; Powell, A. K.; Sessoli, R. *Phys. Rev. Lett.* **2008**, *100*, No. 247205. (b) Lin, P.-H.; Burchell, T. J.; Clérac, R.; Murugesu, M. *Angew. Chem., Int. Ed.* **2008**, *47*, 8848. (c) Lin, P.-H.; Burchell, T. J.; Ungur, L.; Chibotaru, L. F.; Wernsdorfer, W.; Murugesu, M. *Angew. Chem., Int. Ed.* **2009**, *48*, 9489. (d) Layfield, R. A.; McDouall, J. J. W.; Sulway, S. A.; Tuna, F.; Collison, D.; Winpenny, R. E. P. *Chem. Eng. J.* **2010**, *16*, 4442. (e) Xu, G.-F.; Wang, Q.-L.; Gamez, P.; Ma, Y.; Clerac, R.; Tang, J.; Yan, S.-P.; Cheng, P.; Liao, D.-Z. *Chem. Commun.* **2010**, *46*, 1506.
- (4) (a) Felser, C.; Fecher, G. H.; Balke, B. *Angew. Chem., Int. Ed.* **2007**, *46*, 668. (b) Heerdt, P.-T.; Stefan, M.; Goovaerts, E.; Caneschi, A.; Cornia, A. *J. Magn. Reson.* **2006**, *179*, 29. (c) Larsen, F.; McInnes, E.; Mkami, H. E.; Overgaard, J.; Piligkos, S.; Rajaraman, G.; Rentschler, E.; Smith, A.; Smith, G.; Boote, V. *Angew. Chem., Int. Ed.* **2003**, *42*, 101. (d) Costes, J.-P.; Nicodème, F. *Chem.—Eur. J.* **2002**, *8*, 3442. (e) Costes, J.-P.; Dahan, F.; Dupuis, A.; Lagrave, S.; Laurent, J.-P. *Inorg. Chem.* **1998**, *37*, 153. (f) Baril-Robert, F.; Petit, S.; Pilet, G.; Chastanet, G.; Reber, C.;



Luneau, D. *Inorg. Chem.* **2010**, *49*, 10970. (g) Jiang, S.-D.; Wang, B.-W.; Su, G.; Wang, Z.-M.; Gao, S. *Angew. Chem., Int. Ed.* **2010**, *49*, 7448. (h) Matsumoto, Y.; Murakami, M.; Shono, T.; Hasegawa, T.; Fukumura, T.; Kawasaki, M.; Ahmet, P.; Chikyow, T.; Koshihara, S.; Koinuma, H. *Science* **2001**, *291*, 854. (i) Beaulac, R.; Schneider, L.; Archer, P. L.; Bacher, G.; Gamelin, D. R. *Science* **2009**, *325*, 973.

(5) Long, J.; Habib, F.; Lin, P.-H.; Korobkov, I.; Enright, G.; Ungur, L.; Wernsdorfer, W.; Chibotaru, L. F.; Murugesu, M. *J. Am. Chem. Soc.* **2011**, *133*, 5319.

(6) Wernsdorfer, W. *Supercond. Sci. Technol.* **2009**, *22*, 064013.

(7) Gatteschi, D.; Sessoli, R.; Villain, J. *Molecular Nanomagnets*; Oxford University Press: New York, 2006.

(8) (a) Wernsdorfer, W.; Bhaduri, S.; Boskovic, C.; Christou, G.; Hendrickson, D. N. *Phys. Rev. B* **2002**, *65*, No. 180403. (b) Wernsdorfer, W.; Chakov, N. E.; Christou, G. *Phys. Rev. Lett.* **2005**, *95*, No. 037203.

(9) Wernsdorfer, W.; Aliaga-Alcade, N.; Hendrickson, D. N.; Christou, G. *Nature* **2002**, *416*, 406.

(10) (a) Das, A.; Gieb, K.; Krupskaya, Y.; Demeshko, S.; Dechert, S.; Klingeler, R.; Kataev, V.; Büchner, B.; Müller, P.; Meyer, F. *J. Am. Chem. Soc.* **2011**, *133*, 3433. (b) Boskovic, C.; Bircher, R.; Tregenna-Piggott, P. L. W.; Güdel, H. U.; Paulsen, C.; Wernsdorfer, W.; Barra, A.-L.; Khatsko, E.; Neels, A.; Stoeckli-Evans, H. *J. Am. Chem. Soc.* **2003**, *125*, 14046. (c) Bagai, R.; Wernsdorfer, W.; Abboud, K. A.; Christou, G. *J. Am. Chem. Soc.* **2007**, *129*, 12918. (d) Affronte, M.; Lasjaunias, J. C.; Wernsdorfer, W.; Sessoli, R.; Gatteschi, D.; Heath, S. L.; Fort, A.; Rettori, A. *Phys. Rev. B.* **2002**, *66*, No. 064408. (e) Yamaguchi, A.; Kusumi, N.; Ishimoto, H.; Mitamura, H.; Goto, T.; Mori, N.; Nakano, M.; Awaga, K.; Yoo, J.; Hendrickson, D. N.; Christou, G. *J. Phys. Soc. Jpn.* **2002**, *71*, 414.